

A TAGGED PHOTON BEAM AT NAL

BY

P. BIGGS, W. BUSZA, M. CHEN, T. NASH

LABORATORY FOR NUCLEAR SCIENCE, MASSACHUSETTS INSTITUTE OF TECHNOLOGY

AND

THE CANADIAN - M.I.T. COLLABORATION

July 13, 1971

Associated with NAL Proposal #144

INTRODUCTION

We propose the construction of the tagged photon beam shown in Fig. 1. It is expected that up to 200 GeV this beam can produce electron yields, at the tagging target, of greater than  $10^8$  electrons per pulse of  $10^{13}$  incident protons. The contamination from  $\pi^-$  would be less than a few parts in 1000. The photon yield depends on the accuracy to which the photon momentum must be known. For a 0.5% measurement of the photon momentum and a 200 GeV electron beam, for example, one can anticipate about  $3.7 \times 10^5$  photons per pulse in the range 122 GeV to 195 GeV. The beam may be used at higher energies but yields fall below the ones just cited.

With the lead radiator in place and the tagging target removed, one has an electron beam, useful up to about 300 GeV with a momentum acceptance of  $\pm \sim 4\%$  and resolution of  $\pm \sim 0.5\%$  if counter hodoscopes are used to measure the electron momentum.

(A) The Beam

Before going into the details of the yield calculations we will outline the properties and function of each part of the beam. A detailed listing of magnets, their locations and functions may be found in Table 1. Charged particles produced by protons interacting in the Be target are swept away vertically by the following five bending magnets. Photons resulting primarily from neutral pions that were produced by proton interactions proceed to a lead radiator located 75 feet downstream. At the radiator the size of the photon beam is less than about 0.2" in diameter. Charged particles of 500 GeV will have been deflected 7 inches so that they will completely miss the lead radiator. The front edge of the first quadrupole is at 90 feet from the primary target. At this point the minimum that charged particles have been deflected is 10 inches so they safely pass the side of the quadrupole which is 6.5 inches from the center.

In the lead radiator the photons produce  $e^+e^-$  pairs. The electrons are then transported by a three doublet quadrupole system to a tagging target located 968 feet from the primary target. This beam has three foci in both vertical and horizontal planes. Collimators are placed at the first focus to reduce the hadronic component of the beam. At the second focus a counter hodoscope is used to measure the electron momenta to a resolution of  $\pm 0.5\%$ . The experimental target is placed at the third focus which is dispersion free. When a tagged photon beam is desired a tagging target is located after the last beam magnet. A bending magnet can be placed immediately before the tagging target to sweep away low energy charged particles that may have been produced in the last few magnets of the beam. Vacuum is required throughout the beam (except inside the quadrupoles, where helium may be used) to reduce problems from particle interactions along the beam. There will also be a small energy loss of  $\sim 1\%$  due to synchrotron radiation. This will be compensated for by tuning the various segments of the beam to different momenta, decreasing slightly after each bend.

One of the design features of this beam is that the beam spot shape caters to the different requirements of the momentum hodoscope, the tagging system and the experimental target at the three locations. At the momentum hodoscope the beam is 3.0 inches wide and about 3 inches high. A spatial measurement of 0.5 cm horizontally at this point gives  $\pm 0.5\%$  momentum resolution. At the tagging target the beam spot is 3 inches wide and 0.4 inches high at its maximum extent. This size fits neatly into the aperture of the tagging magnet. This shape also facilitates the design of the tagging system. At the experimental target the beam spot is narrow and high (0.4 inches x 2.5 inches). It, therefore, allows a good measurement of the horizontal photon direction for those reactions where experimental deduction of the vertex position is not possible. It, also, facilitates measurement of the parameters of the low momentum recoil protons.

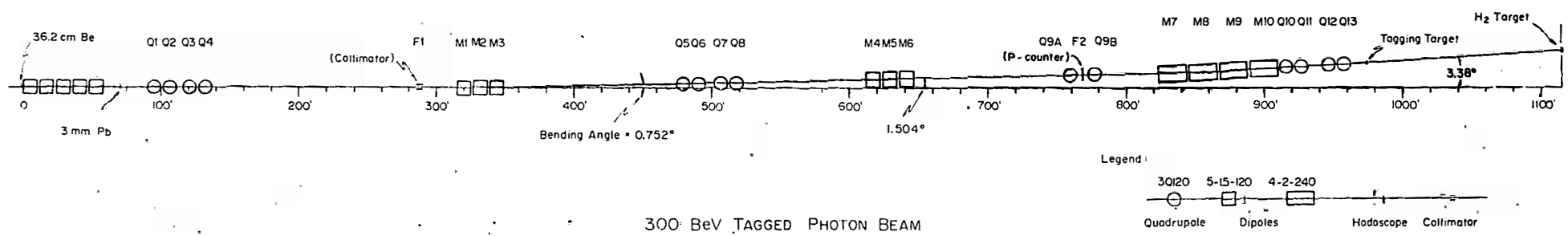


Fig.1

Table 1

## TABLE OF MAGNETS, TARGETS AND COLLIMATORS FOR TAGGED PHOTON BEAM

Position (ft)	Element Name	Element Code	Field Strength	Function
0	Be target			Produce $\gamma$ rays
6		5 - 1.5 - 120	14.58 kG	
17		5 - 1.5 - 120	14.58 kG	Sweep p and other charged particles away from the neutral beam
28		5 - 1.5 - 120	14.58 kG	
39		5 - 1.5 - 120	14.58 kG	
50		5 - 1.5 - 120	14.58 kG	
75	Radiator			Convert $\gamma$ into $e^+$
95	Q1	3Q - 120	- 6.856 kG/1.5"	
106	Q2	3Q - 120	- 6.856 kG/1.5"	
121	Q3	3Q - 120	+ 6.306 kG/1.5"	Doublet 1
132	Q4	3Q - 120	+ 6.306 kG/1.5"	
287	Collimator			Reject $\pi^-$
320	M1	5 - 1.5 - 120	14.58 kG	
332	M2	5 - 1.5 - 120	14.58 kG	Bend $e^-$ away from initial production direction
344	M3	5 - 1.5 - 120	14.58 kG	
479	Q5	3Q - 120	+ 4.658 kG/1.5"	
490	Q6	3Q - 120	+ 4.658 kG/1.5"	Doublet

Table 1 continued

Position (ft)	Element Name	Element Code	Field Strength	Function
506	Q7	3Q - 120	- 4.530 kG/1.5"	Doublet
517	Q8	3Q - 120	- 4.530 kG/1.5"	
615.3	M4	5 - 1.5 - 120	14.58 kG	Produce dispersion at p-counter
627.3	M5	5 - 1.5 - 120	14.58 kG	
639.3	M6	5 - 1.5 - 120	14.58 kG	
759.3	Q9A	3Q - 120	7.578/1.5"	Field lens
768.3	P counter			Measure the e <sup>-</sup> momentum
777.3	Q9B	3Q - 120	- 2.872 kG/1.5"	Field lens
834.3	M7	4 - 2 - 240	10.6 kG	Make achromatic beam after Q13
856.3	M8	4 - 2 - 240	10.6 kG	
878.3	M9	4 - 2 - 240	10.6 kG	
899.3	M10	4 - 2 - 240	10.6 kG	
915.3	Q10	3Q - 120	- 5.348 kG/1.5"	
926.3	Q11	3Q - 120	- 5.348 kG/1.5"	Doublet
945.3	Q12	3Q - 120	+ 5.15 kG/1.5"	
956.3	Q13	3Q - 120	+ 5.15 kG/1.5"	
968.3	Tagging target			Produce tagged photons
	Tagging mag A	CEA H mag	18 kG	Measure the energy of the scattered e <sup>-</sup>
	Tagging mag B	CEA C mag	18 kG	
1122.3	Experimental target			

(B) The Monte Carlo Calculations

All the Monte Carlo calculations used the theoretical yield predictions of pions and protons off lead and Be from the thermodynamical model of Hagedorn and Ranft<sup>1</sup> as calculated by Ranft's program SPUKJ. The latest parameters (October 1970)<sup>2</sup> were used. These theoretical extrapolations to high energy are only expected to be good to a factor of two or so. As new measurements at high energy are made and the extrapolations are improved we shall, in turn, update our calculations.

The electron yield calculations assume the following sequence of events:

- a. proton beam passing through Be is attenuated;
- b. proton interaction produces a neutral pion which decays isotropically, in its rest frame, into two photons;
- c. the photon intensity is attenuated in the Be by pair production;
- d. photons travel to Pb radiator where their intensity is attenuated;
- e. photons produce  $e^+e^-$ ;
- f.  $e^-$  loses energy by bremsstrahlung (Bethe-Heitler straggling formula used in the integral relations of Tsai and Whitis<sup>3</sup>) and is deflected by multiple scattering;
- g.  $e^-$  goes down beam line if accepted by the transport system.

The pion background calculations assume the following sequence of events:

- a. proton beam passing through Be is attenuated;
- b. proton interaction produces a neutron;
- c. neutrons are attenuated in passing through the rest of the Be;
- d. neutrons travel to Pb radiator where their intensity is attenuated;
- e. neutrons produce negative pions which are multiply scattered and attenuated while traversing the remainder of the radiator;



f. the pion goes down beam line if accepted.

Assuming the theoretical yield predictions are correct, these calculations are, if anything, conservative. In calculating the electron rate, other photon producing processes in the Be besides neutral pion production are ignored. In calculating the  $\pi^-$  contamination, proton induced proton yields in Be were used since there are no thermodynamic model predictions of neutron yields. This is an overestimate at highenergies and small angles, since elastic reactions not possible for neutrons are included.

(C) The production target and the converter:

(1) The production of  $\pi^0$ 's by protons

One may analytically determine the optimum primary target thickness. For Be a peak occurs in the relative yields at a thickness of 1.21 collision lengths (36.3 cm). The pion background ratio increases slowly with thickness. Beyond 1.21 collision lengths the photon yield decreases because of radiative attenuation. The peak of 1.21 collision lengths was therefore selected as the best thickness to use for Be and this has been included in the Monte Carlo calculations.

Be was used in these calculations as the target material because of the ease of handling it. It is a metal. It has low collision length to radiation length ratio. In fact, this ratio is yet another factor of four smaller for deuterium. By using deuterium as target one increases the yield of electrons by up to a factor of two while simultaneously reducing the pion contamination fraction in the beam by about 15%. A factor of 1.47 of this factor results directly from the long radiation length of deuterium so that the peak where radiative attenuation starts to cut in comes at 1.95 collision lengths (versus 1.21 for Be). A further factor of about 1.3 comes from the higher pion yields per collision length for protons on deuterium compared with protons on Be. The length of the deuterium target would be 1.95 collision lengths or 394 cm. This added length poses no problem from the standpoint of the focussing properties of the beam. Since the angular acceptance of the beam is about 1 mr, photons coming from one end or the other of the  $D_2$  target would appear to come from a spot of radius about .08" at the centre of the target. This small increase in spot size causes only a small loss of events at high energies where the effective spot size is small. At low energies, where multiple scattering in the target causes the effective spot size to be larger than

.08" there is no loss of rate due to the length of the  $D_2$  target. One expects a gain, over Be, of at least a factor of 2 up to 100 GeV and 1.5 at 200 GeV. Because of the small size of the beam the target need only be about 1 cm in diameter. Such dimensions (4 meters x 1 cm), though unusual, seem feasible. The gain in rate should more than pay for the expense of such a target by reducing the required running time for experiments using the beam.

(II) Conversion of  $\gamma$  rays into electrons

Lead is used because of its extremely high collision length to radiation length ratio. This reduces the pion background relative to the electrons.

The Monte Carlo calculations make no thin radiator approximation and are therefore good for thick targets. Included in Figs. 2 and 3 are results for four radiator thicknesses. These numbers and the more precise results for a 200 GeV beam show that the electron yields reach a plateau at about 0.5 radiation lengths and that the pion contamination fraction appears to rise with lead radiator thickness. It therefore seems most reasonable to use a 0.5 radiation length (0.29 cm) lead radiator.

Electron Yields and Background Ratio vs Energy and Radiator Thickness

36.2 cm Be target  
No proton deflection

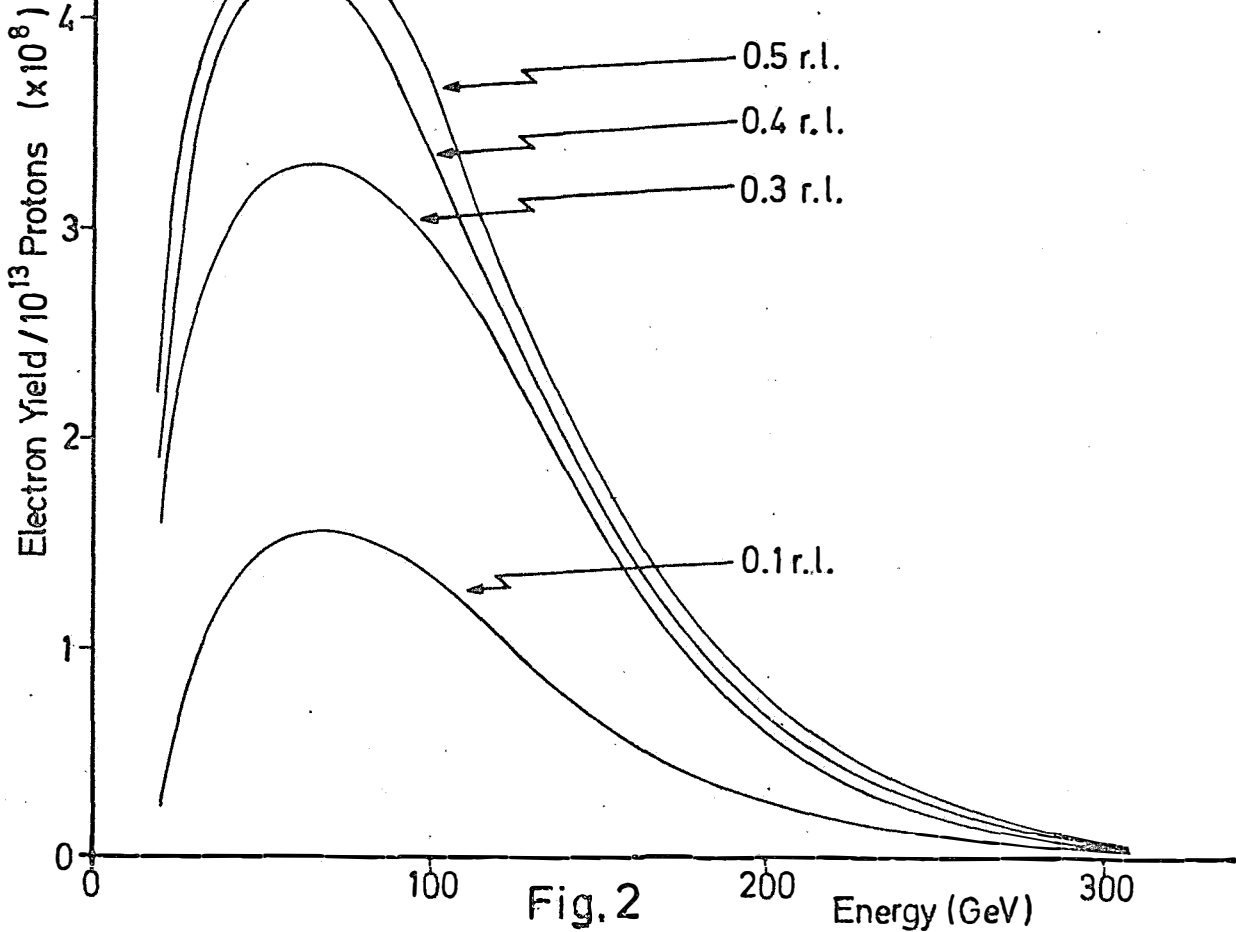
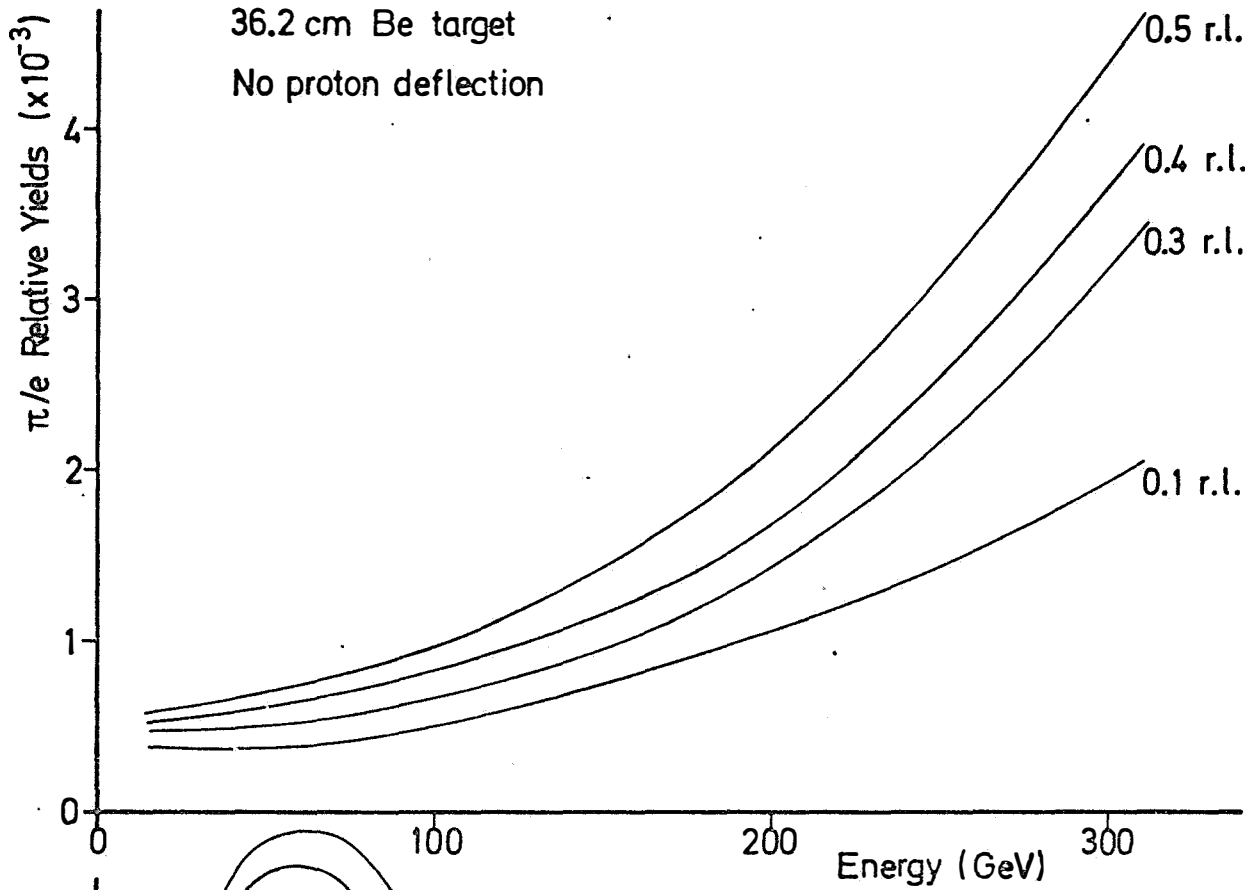


Fig. 2

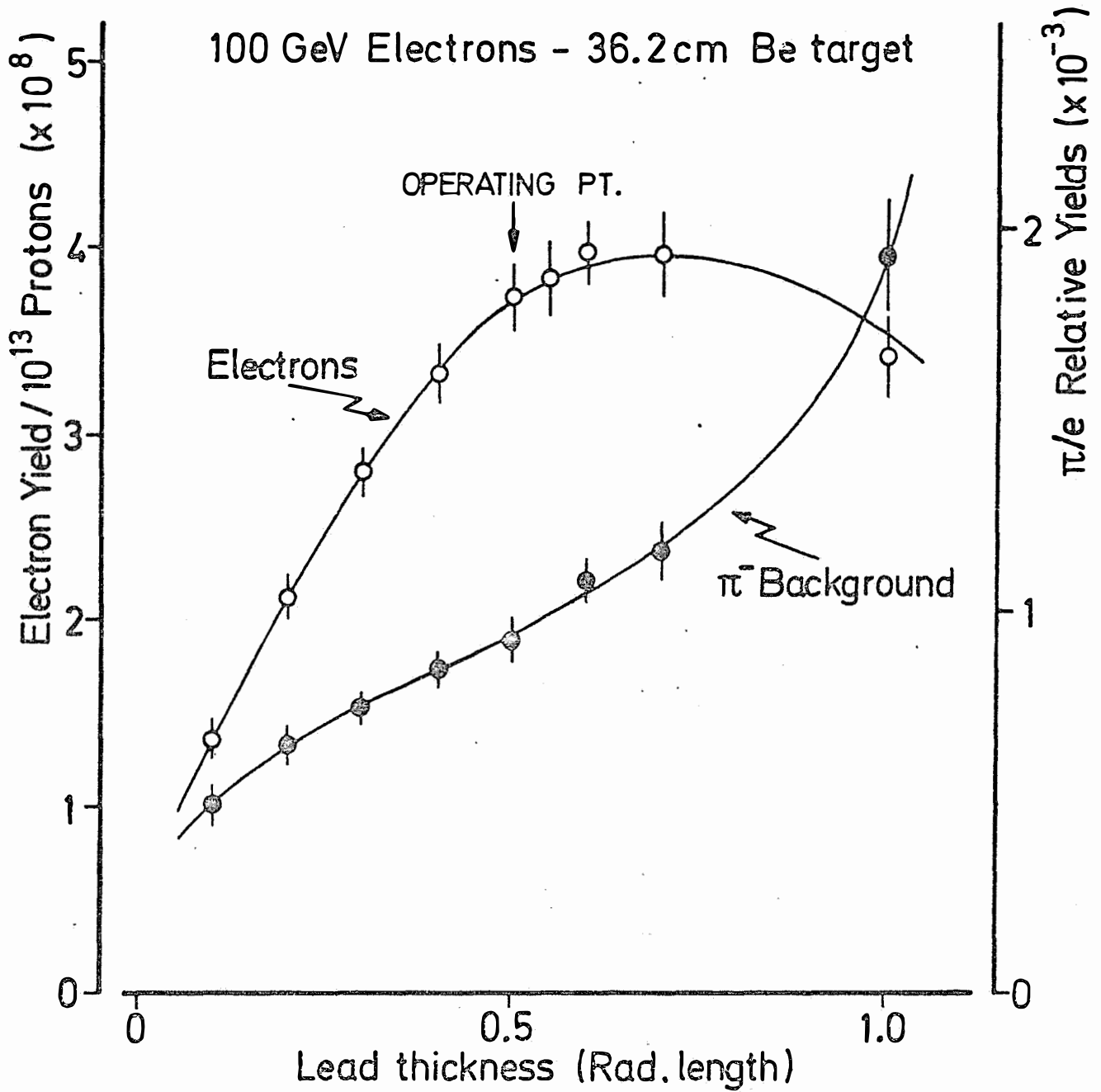


Fig. 3

(D) The Pion Contamination

The pions in the beam result from neutrons produced by protons interacting in the primary target. These neutrons cannot be swept away from the photon beam heading for the lead radiator. In the radiator the neutrons produce negative pions which are transported by the beam along with the electrons. There are two ways of keeping this contamination at the acceptable level of less than one part in a thousand. The first approach makes use of the fact that the virtual source size at the primary target as seen by the beam magnets is much larger for the pions than for the electrons. The electrons are produced in the radiator at very small angles ( $\sim 0.1$  mr at 200 GeV) from the direction of the photon. They are further deflected by a small angle of about the same size by multiple scattering. Thus the electrons appear to come from a spot at the primary target that is not significantly larger than the size of the proton beam (which is assumed to have radius of about .04 inches). On the other hand, the cross-section for pion production by neutrons in lead remains high at angles significantly larger than these. The pions therefore appear to come from a much larger spot in the primary target (see Fig. 4). At the foci of the beam the electron spot will be surrounded by a pion halo. Thus by using collimators at these points one may reduce the pion contamination. Since the pion contamination does not seem to be serious at present the collimators are placed just at the edges of the electron spatial distributions at each of the foci in order to cut pions without reducing the electron yield. The result of the detailed calculation of  $\pi$  contamination in the beam is shown in Figs. 2 and 3. If it turns out that the contamination is more serious than we now expect on the basis of theoretical extrapolations to these energies, then these collimators may be tightened up, thus

reducing both the pion contamination and the electron yield further.

If necessary a second method of reducing the background may be used. The neutron yields at the primary target fall off more rapidly with angle than do the  $\pi^0$  (and hence the resulting photon) yields. Thus by deflecting the incoming proton beam by a few milliradians a further reduction of background is possible. This is the function of the three bending magnets located just before the primary proton target. Calculations of the effect of a horizontal proton deflection of 2 mr are shown in Fig. 5.

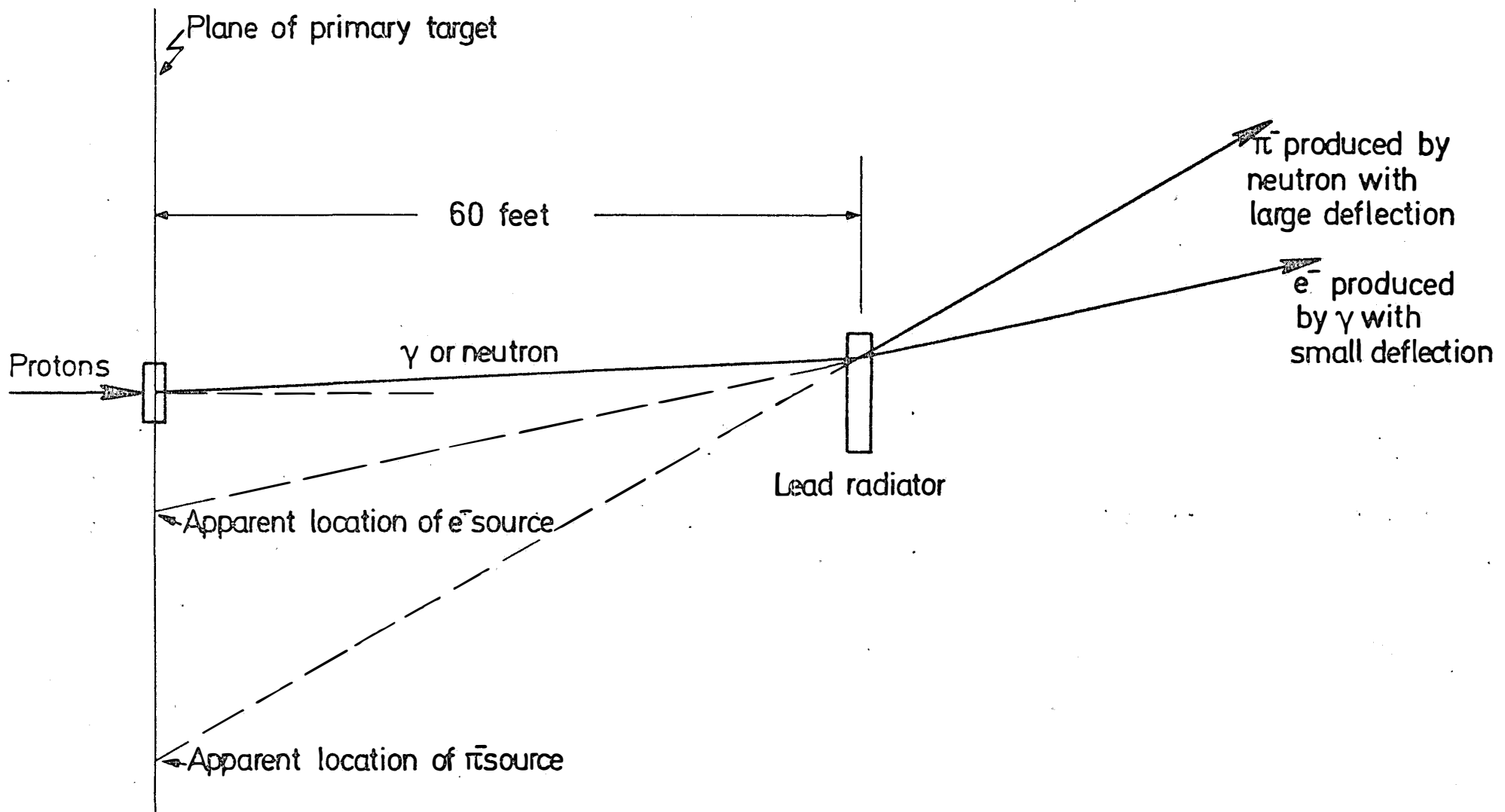


Fig. 4



### Electron Yields and Background Ratio vs Energy and Radiator Thickness

36.2 cm Be target

Proton deflection = 2 mr horizontal

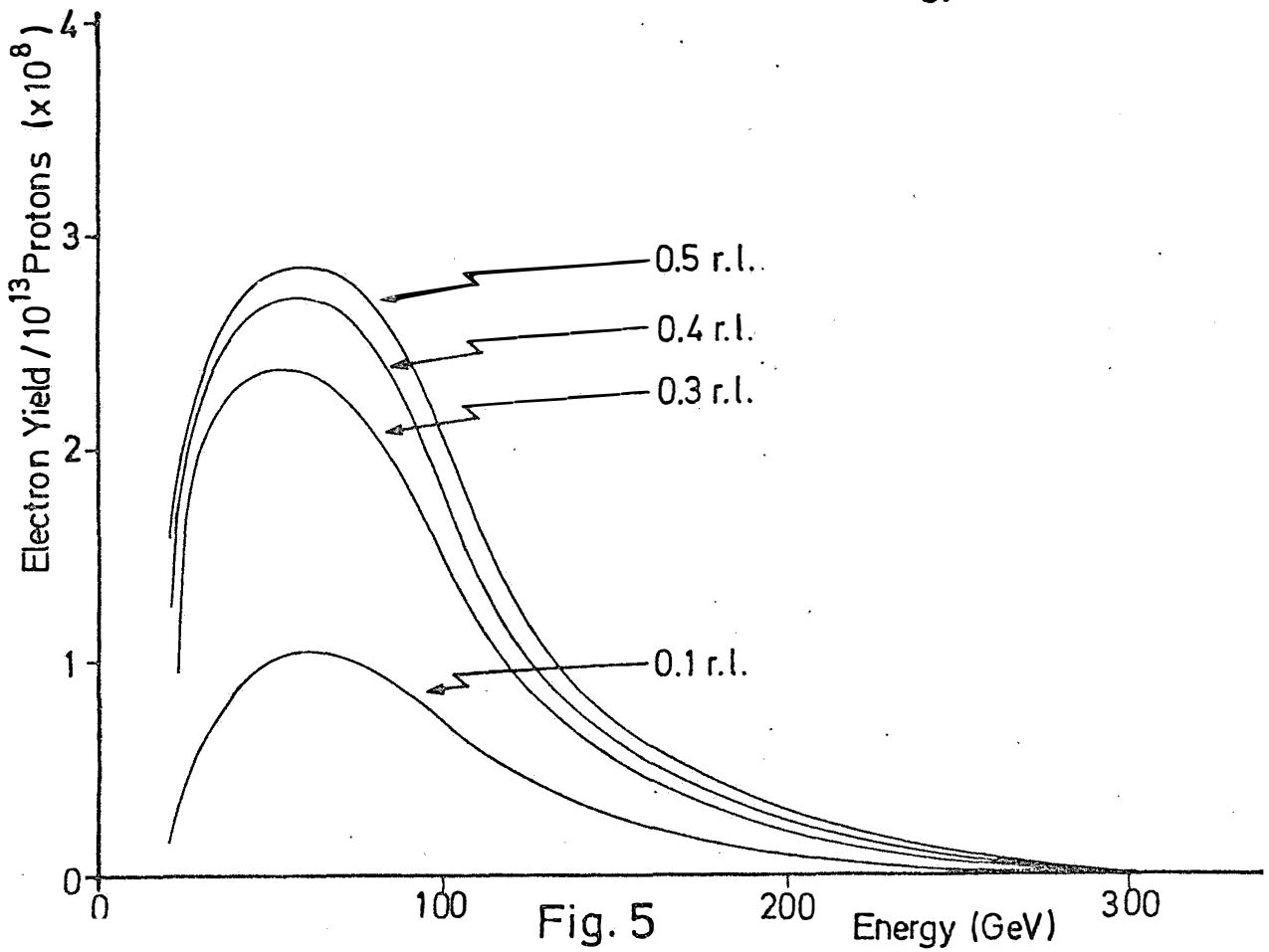
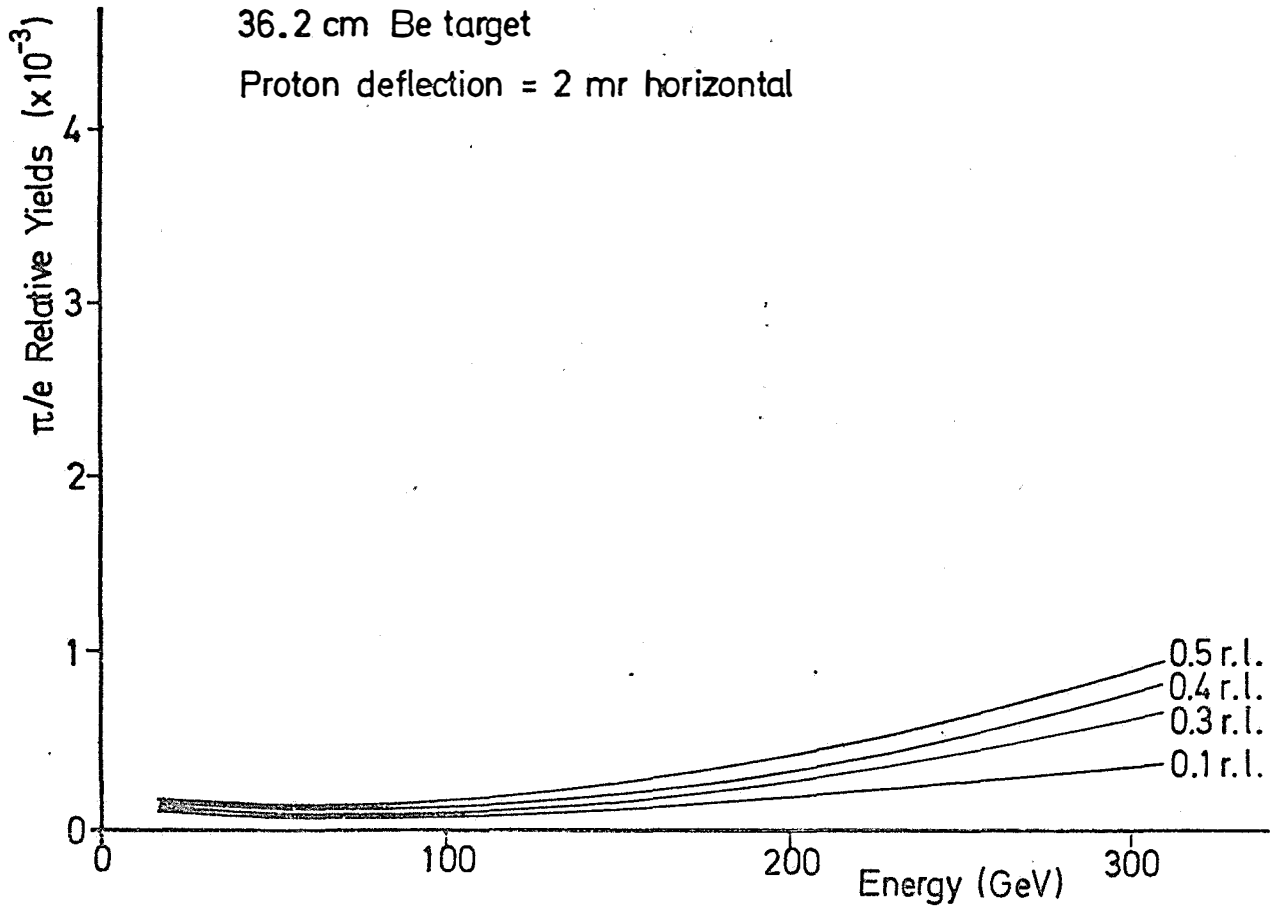


Fig. 5

(E) The tagging system

The tagging system (shown in Fig. 6) is designed with available Cambridge Electron Accelerator magnets, and operated at a total of 0.25 MW power. The tagging target is a 0.5 mm (0.01 r.l.) thick lead sheet. The electrons radiate in the target and produce photons. The recoiling electron is momentum analyzed by a series of magnets. The photon beam proceeds unaffected through the magnets to the experimental target. From the knowledge of the momentum of the electron before and after passing through the tagging radiator, the momentum of the photon is deduced. The CEA tagging magnets used here consist of two H type magnets of the dimension 48" x 16" x 5" each, and one C type magnet of the dimension 72" x 10" x 4". All of these magnets are presently on the floor of CEA and may be available to us.

The vertical size of the beam spot is  $\pm 0.2''$  at the tagging target. The interaction point inside the  $H_2$  target, which is 140' downstream from the tagging target, can be located to an accuracy of  $\pm 0.2''$ . Therefore, the incident electron direction and the outgoing photon direction are known to an accuracy better than 0.2 mr in the vertical plane.

Behind the tagging magnets there are two proportional chambers to measure the vertical positions of the scattered electron. This information, together with a knowledge of the initial electron direction and energy, determines the scattered electron energy, and, therefore, the tagged photon energy. The photon energy resolution is shown in Table 2.

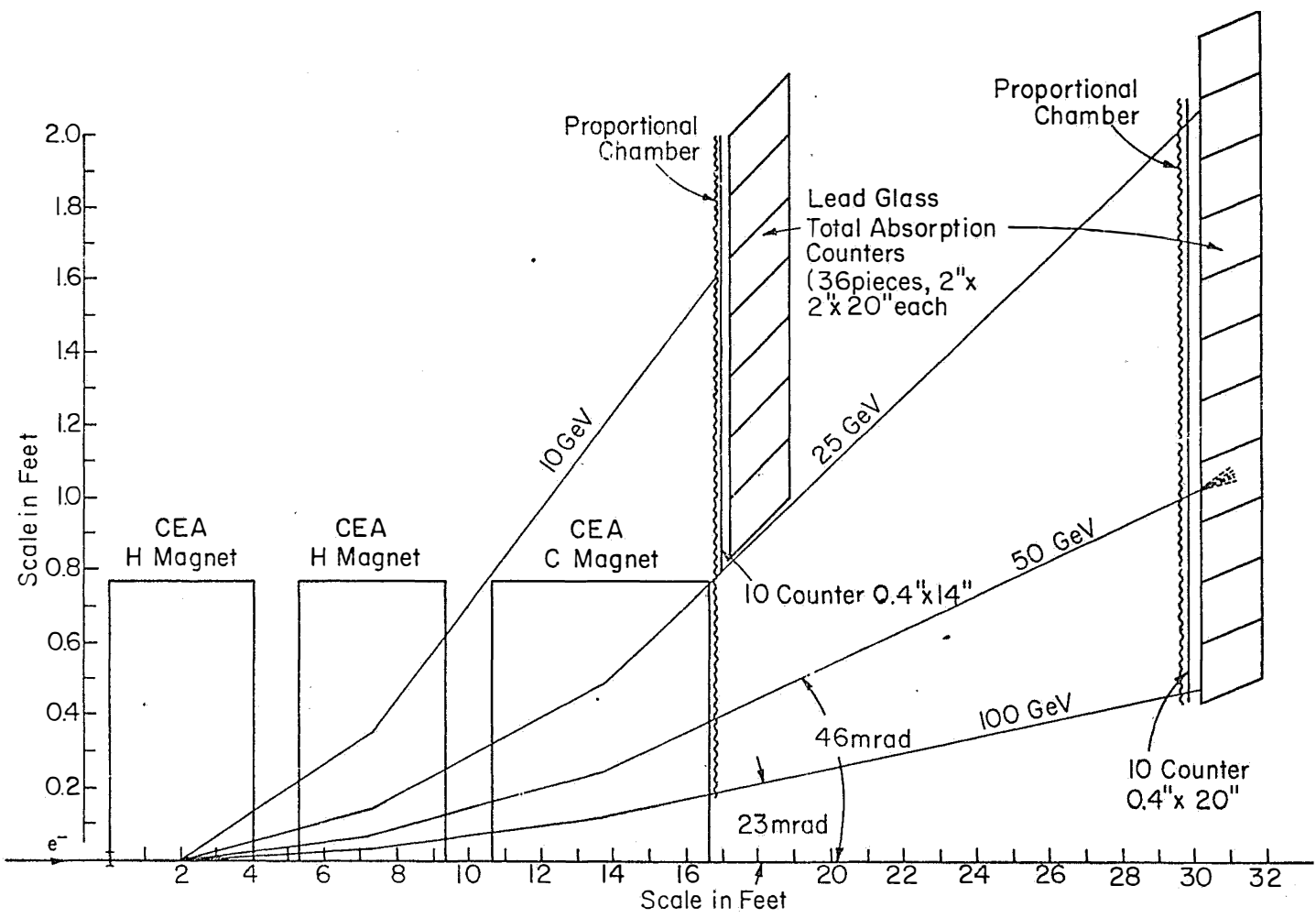
There are 10 hodoscope counters behind each of the chambers. These hodoscopes determine

- a. whether a tagged photon was emitted,
- b. when the photon (or the event) occurred, and
- c. the horizontal position of the incident electron,

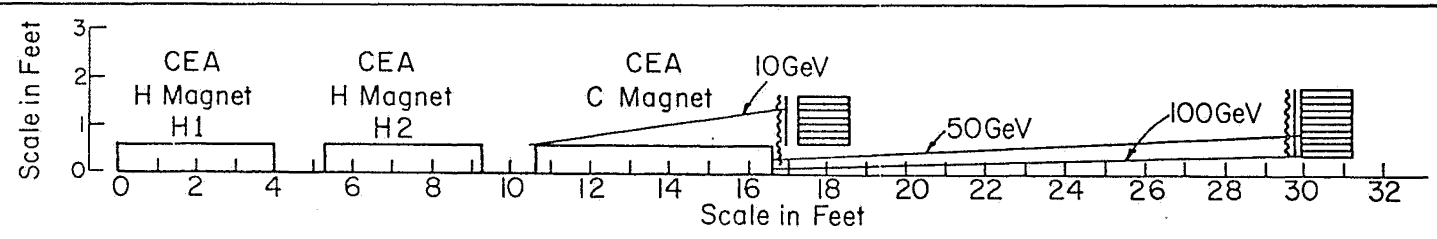
and therefore the horizontal angle  $\theta$  of the emitted photon.

Forty lead glass counters of the size 2" x 2" x 20" situated behind the hodoscope counters measure the pulse height of the scattered electron to reject pions and low-energy electrons. The lead glass counter enables an additional  $\pi/e$  rejection of 100, giving the total  $\pi/e$  rejection of the tagged photon beam to  $\sim 10^{-5}$ .

Expected photon yields for 200 GeV incident electron energy with  $10^8$  electrons/pulse and 0.01 radiation length radiator is  $4 \times 10^5$ . If the primary proton beam energy is 300 GeV instead of 500 GeV, one can obtain the approximate  $e^-$  flux rate from Fig. 3 or Fig. 4 by multiplying the electron energy by 0.45.



a)



b)

Fig. 6

Table 2

ENERGY RESOLUTION OF TAGGED PHOTON

Energy of Incident electron:  $E = 200$  GeV

Energy of Scattered Electron $E'$ (GeV)	Bending Angle of Electrons $\theta$ (mr)	Energy of Photons $E_\gamma$ (GeV)	$\frac{\delta E_\gamma}{E_\gamma}$
100	23	100	$\pm 1.7\%$
50	46	150	$\pm 0.6\%$
25	92	175	$\pm 0.5\%$
10	130	190	$\pm 0.5\%$

Acknowledgements:

We wish to acknowledge important discussions with the NAL staff members, in particular Dr. Lincoln Read and Dr. A.W. Maschke, and Prof. D. Reeder.

REFERENCES

1. R. Hagedorn and J. Ranft, Suppl. Nuovo Cimento 6, 169 (1968).  
J. Ranft, RHEL/R 165 (1968).  
J. Ranft, Phys. Letters 31 B, 529 (1970).  
(For further references see Ref. 2).
2. CERN Computer Center, Program Library, Program W 129, Long Write up.